Published in final edited form as:

Neuron. 1996 October ; 17(4): 627–640.

Regulation of Synapse Structure and Function by the Drosophila Tumor Suppressor Gene *dlg*

Vivian Budnik[*], **Young-Ho Koh**[*], **Bo Guan**[*], **Beate Hartmann**[*], **Colleen Hough**[†], **Daniel Woods**[†], and **Michael Gorczyca**[*]

[*]Department of Biology, University of Massachusetts, Amherst, Massachusetts 01003

[†]Developmental Biology Center, University of California, Irvine, California 92717

Summary

Mutations of the tumor suppressor gene *discs-large (dlg)* lead to postsynaptic structural defects. Here, we report that mutations in *dlg* also result in larger synaptic currents at fly neuromuscular junctions. By selectively targeting DLG protein to either muscles or motorneurons using *Gal-4* enhancer trap lines, we were able to rescue substantially the reduced postsynaptic structure in mutants. Rescue of the physiological defect was accomplished by presynaptic, but not post-synaptic targeting, consistent with our finding that miniature excitatory junctional currents were not changed in *dlg* mutants. These results suggest that DLG functions in the regulation of neurotransmitter release and postsynaptic structure. We propose that DLG is an integral part of a mechanism by which changes in both neurotransmitter release and synapse structure are accomplished during development and plasticity.

Introduction

The mechanisms by which synapses assemble and function have been a topic of considerable interest for many years (Fallon and Hall, 1994). Equally intriguing are the synaptic mechanisms that provide for functional and structural flexibility during development and plasticity. Examples of this flexibility have been widely documented. A classical example is the development and regeneration of the retinotectal system of vertebrates, in which a rough retinotopic map is initially established. This rough map is later refined to give rise to the final mature pattern of connectivity (reviewed by Goodman and Shatz, 1993). Similarly, changes in synapse structure and function are observed during postembryonic development of motor systems. In mice, frogs, crayfish, and flies, target muscles continue to grow for relatively long periods after synaptogenesis (Atwood and Kwan, 1976; Gorczyca et al., 1993; Hall and Sanes, 1993). Since these muscles are continuously functional, there must be mechanisms that adjust the size or physiological properties of the pre- and postsynaptic junction, to ensure that motorneurons can drive their growing target muscles (e.g., Lnenicka and Atwood, 1985).

Correspondence should be addressed to V. B.

At the behavioral level, along-lasting change in neuro-transmitter release is believed to underlie the process of learning and memory. Ultrastructural changes at individual synapses are suggested to accompany this functional change (Genisman et al., 1993; Weiler et al., 1995). Understanding the cellular and molecular mechanisms that allow synaptic flexibility is crucial to our understanding of how nervous systems develop and function. The discovery that at least some synaptic elements, such as the N-methyl-D-aspartic acid (NMDA) receptor, are involved in both functional and structural plasticity (Schmidt, 1990) suggests that factors must exist that mediate interactions between ion channels and neuro-transmitter receptors, and the synaptic cytoskeleton.

The MAGUK family of proteins (membrane-associated guanylate kinase homologs; Woods and Bryant, 1993) may be involved in the signaling cascades that link changes in excitability to changes in synapse structure. MAGUKs are multidomain proteins characterized by the presence of one to several PDZ domains (also known as discs-large homologous region [DHR] domains) believed to mediate direct interactions with ion channels and receptors (Doyle et al., 1996), an *src*-homology region 3 (SH3) domain, and a guanylate kinase (GUK) domain (reviewed by Budnik, 1996). A mammalian member of this family is the synaptic protein PSD-95/SAP-90 (Cho et al., 1992; Kistner et al., 1993). In the hippocampus, this protein is found at the postsynaptic density and binds directly to the cytoplasmic tail of the NMDA receptor (Cho et al., 1992; Kornau et al., 1995). In addition, PSD-95/SAP-90 is involved in clustering these channels and in interactions with the cellular cytoskele-ton (Cho et al., 1992; Kim et al., 1995, 1996). These interactions raise the interesting possibility that in the nervous system MAGUKs may be involved in structural and perhaps functional plasticity.

A Drosophila MAGUK is the tumor suppressor gene *discs-large* (*dlg*). In epithelial tissues, DLG is expressed at septate junctions, and in the nervous system at central and peripheral synapses (Woods and Bryant, 1991; Lahey et al., 1994). Mutations in *dlg* lead to the formation of neoplastic tumors in epithelial and neural tissues, and flies die at late larval stages or early metamorphosis. However, DLG protein has a maternal component that provides some phenotype protection. In embryos lacking both the maternal and zygotic components, generated by germline clones, absence of DLG induces more serious alterations, including abnormal dorsal closure and head involution, and neurogenic defects (Perrimon, 1988).

The neuromuscular junction of Drosophila is one model system to examine the mechanisms by which MAGUKs or other factors influence synapse assembly and maturation (Lahey et al., 1994). Body wall muscles of larvae are innervated by at least three classes of structurally different neuromuscular endings. Type I boutons innervate all muscle fibers and are responsible for classical chemical synaptic transmission mediated by glutamate (Jan and Jan, 1976; Johansen et al., 1989). Type II boutons contain octopamine and innervate all but eight body wall muscles (Monastirioti et al., 1995). A third class of boutons contains peptides, such as proctolin, insulin-like peptide, or leucokinin I (Anderson et al., 1988; Cantera and Na¨ssel, 1992; Gorczyca et al., 1993), and innervate discrete populations of muscle fibers. Each of these motor endings can be uniquely identified by its morphological and

neurotransmitter phenotypes, and some bouton types can be distinguished electrophysiologically.

At the Drosophila neuromuscular junction, *dlg* is expressed primarily at the pre- and postsynaptic membrane of Type I boutons (Lahey et al., 1994). At the postsynaptic region, it is associated with a postsynaptic specialization, the subsynaptic reticulum (SSR). The SSR consists of highly elaborated junctional membranes that surround Type I boutons (Jia et al., 1993). Hypomorphic mutations in *dlg* result in a poorly developed and much simpler SSR (Lahey et al., 1994). Developmental studies show that in wild type, the surface of this post-synaptic structure increases (about 100-fold) as the target muscle cell becomes larger (over 100 times in volume) during larval growth (Guan et al., 1996). In the mutant, the SSR forms normally at initial larval stages, but fails to expand as target muscles grow. These results support the model that suggests that *dlg* is involved in adjusting the size of postsynaptic surfaces during development.

In the current paper, we tested the hypothesis that DLG is involved in the regulation of synaptic surface size, by selectively modifying the levels of DLG in the pre- and postsynaptic cell in wild type and *dlg* mutants. This was accomplished by using *Gal-4* enhancer traps (Brand and Perrimon, 1993), with specific expression of the yeast transcriptional activator Gal-4 in identified motorneurons or muscles. These synapse- and muscle-specific *Gal-4* strains were then used to drive the expression of *dlg* cDNA. Our results show that selective expression of *dlg* in either the pre- or postsynaptic cell substantially rescues the mutant phenotype at the SSR.

To examine the functional significance of *dlg* in the physiology of neuromuscular junctions, we used voltage clamp techniques to study the properties of excitatory junctional currents (EJCs). We found that stimulation of motorneurons in two *dlg* mutant alleles resulted in an abnormally large EJC. This defect was likely to be the result of an increased neurotransmitter release, as demonstrated by analysis of miniature EJCs, determination of quantal content, and analysis of *dlg* mutant strains with selective *dlg* expression at Type I motorneurons or muscles. These results support the hypothesis that *dlg* is involved in the regulation of both synapse structure and function.

Results

dlg Targeting Using *Gal-4* Enhancer Traps

Previous studies have demonstrated that *dlg* is required for normal development of Type I bouton postsynaptic structure (Lahey et al., 1994). In the presence of altered DLG protein, the SSR at the postsynaptic junctional region is simpler (less folded and with reduced number of membrane layers) than in larvae with normal DLG. A small but significant reduction in vesicle density is observed in dlg^{m52}/Df, but no other presynaptic abnormalities are seen in the *dlg* mutant alleles studied (Table 1). To determine the contribution of postsynaptically expressed DLG to the development of the SSR, we used muscle-specific *Gal-4* enhancer traps to drive *UAS-dlg*. *UAS-dlg* was constructed by subcloning a *dlg-A* cDNA, which contains the coding sequence for the *dlg-A* transcript (Woods and Bryant,

1991), into the pUAST vector (Brand and Perrimon, 1993). Four independent *UAS-dlg* transformants were obtained by germline transformation.

To drive *dlg* in body wall muscles, we used two P[*Gal-4*] insertions, BG487 and BG57. BG487 has a strong anteroposterior gradient of Gal-4 expression in a subset of body wall muscles, starting at muscle 31 in abdominal segment 1 (A1) and decreasing in muscles 6 and 7 of every abdominal segment. This pattern of Gal-4 expression can be visualized by anti-β-galactosidase (βgal) staining in BG487/UAS–*LacZ* larvae (Figure 1A). No or very low levels of anti-βgal immunoreactivity were detected in muscles other than 6 and 7 in A2-A8. About five sensory cell bodies per hemisegment also displayed strong Gal-4 expression in the body wall. These sensory cell bodies sent axons into the CNS neuropil; however, no cell bodies had Gal-4 expression within the CNS (data not shown). Except for salivary glands, which express Gal-4 in nearly all enhancer traps, no other tissues had detectable βgal immunoreactivity in the larva. This pattern of Gal-4 expression was identical throughout larval development (first to third instar), and no expression was seen in the embryonic stages.

BG57, in contrast, expressed Gal-4 in all larval muscles, from mid first to third instar stage (Figure 1E). In addition to muscles, Gal-4 expression was observed in two sensory cell bodies in the body wall and in other mesodermally derived tissues, such as the gut. No expression was seen in ectodermal tissues, such as cuticle and CNS (with the exception of few incoming sensory axons). Thus, BG487 and BG57 allowed us to target postsynaptic *dlg* expression through most of the life of Type I synapses.

Postsynaptic *dlg* Partially Rescues the Mutant Phenotype at Type I Synapses

To determine if postsynaptic expression of *dlg* would restore the structural defects of the SSR in *dlg* mutants, we examined body wall muscles from dlg^{m52}*/Df;* BG487/ UAS-*dlg* (*dlg^{m52}; post-dlg*) larvae. These mutant larvae contain one copy of BG487 and one copy of *UAS-dlg*. As previously demonstrated, DLG immunoreactivity in dlg^{m52}/Df synapses is barely above background. In $dlgm^{52}$*; post-dlg*, DLG immunoreactivity was intense around Type I synapses in muscles 6 and 7 (A2-A7), but not in Type I synapses of other muscles (compare Figures 1C and 1D). This result confirms the ability of BG487 to drive *UAS-dlg* specifically in muscles 6 and 7. Unlike βgal immunoreactivity, the DLG label was concentrated around Type I boutons and was not observed at other muscle regions.

There are two Type I bouton classes that have been described at the body wall, Type I_s (small) and Type I_b (big) (Atwood et al., 1993; Jia et al., 1993; Kurdyak et al., 1995). Both bouton types release glutamate, but they differ in their morphology and physiology. Type I_b boutons are larger, have an extensive SSR at the postsynaptic region, and give rise to smaller amplitude EJCs. Type I_s boutons have a reduced SSR and give rise to larger amplitude EJCs. Both bouton types stain with anti-DLG antibodies, but the staining is significantly stronger at Type I_b boutons (Lahey et al., 1994). In dlg^{m52}*; post-dlg*, DLG immunoreactivity concentrated around both Type I_b and Type I_s (data not shown).

Muscles 6 and 7 are innervated only by Type I boutons. However, muscle fiber 31 (present in A1), which also expresses Gal-4 in BG487 larvae, is innervated by both Type I and the

smaller Type II boutons (Figure 1B). Type II boutons contain both glutamate and octopamine and are devoid of SSR (Jia et al., 1993; Monastirioti et al., 1995). This presented an ideal opportunity to test the bouton specificity of the UAS–*dlg* construct. Postsynaptic *dlg* targeting to muscle fiber 31 in dlg^{m52}*; post-dlg* still resulted in accumulation of DLG immunoreactivity solely around Type I boutons. No immunoreactivity was observed at Type II boutons. Similar results were obtained with the BG57 *Gal-4* strain(Figure 1F). Thus, when *dlg* is driven by Gal-4 in BG487 or BG57, its product is targeted to the normal junctional region in the postsynaptic muscle cell. Moreover, this localization is specifically directed to the Type I bouton junctional region, even when another bouton type innervates the same muscle cell.

As mentioned above, at the light microscopical level, postsynaptic *dlg* targeting in the mutant appeared to restore to normal the level of DLG immunoreactivity (Figures 1C, 1D, and 1F). However, it was also important to test whether postsynaptic DLG targeting could rescue the fine structure of Type I synapses. In normal neuro-muscular junctions, DLG immunoreactivity surrounds Type I boutons, but in a non-homogenous fashion, defining a perisynaptic network probably representing the SSR (Lahey et al., 1994). In *dlg* mutant alleles, in which abnormal DLG protein is produced (Woods and Bryant, 1991), anti-DLG immunoreactivity around Type I boutons is less extensive and is devoid of perisynaptic network. We found that in dlg^{m52}*; post-dlg* larvae, in which DLG is driven in muscles 6 and 7, Type I boutons had an appearance that was intermediate between the wild type and mutants. This change, however, could represent simply an increase in the amount of DLG around Type I boutons or a partial rescue of the structural abnormalities in the mutant (or both).

To confirm that the fine structure of Type I boutons was indeed partially rescued in dlg^{m52}*; post-dlg*, an electron microscopy (EM) analysis was conducted (Figures 2A, 2B, and 2D; Figure 3). In wild-type body wall muscles, Type I boutons are surrounded by the SSR, which during the third larval instar is composed of many layers of highly folded membranes provided by the muscle (Figure 2A). In *dlg* mutants, the SSR forms, but is significantly less developed than in wild type, being less extensive and simpler and lacking the typical folded appearance observed in the wild-type SSR (Figure 2B; Lahey et al., 1994). Postsynaptic DLG targeting in a mutant background, using BG487, resulted in an SSR that was more extensive and folded than the mutant (Figure 2D). Unlike wild type, however, its membrane layers appeared less compact or more loosely arranged around the bouton.

To quantitate these changes, we traced the SSR, measured its cross-sectional length, thickness (distance between the presynaptic membrane and the distal limit of the SSR), density (number of membrane layers/μm), and index of convolution (percentage of membrane segments at an angle between 45° and 135° with regard to the presynaptic membrane in an area of 0.5 μm^2) (Figure 3). To correct for differences in bouton size, the SSR cross-sectional length and thickness were normalized by the bouton cross-sectional area as in Lahey et al. (1994). As previously shown, wild-type SSR was about 40% larger in normalized cross-sectional length and thickness than *dlg* mutants (SSR length = 61.8 ± 8.2 μm^{-1} in wild type versus 36.0 ± 4.2 μm^{-1} in dlg^{v59}, and 40.6 ± 3.3 in dlg^{m52}, $p < 0.001$; SSR thickness = 0.22 ± 0.04 μm^{-1} in wild type versus 0.15 ± 0.03 μm^{-1} in dlg^{v59} and 0.17 ± 0.02

in *dlg*^{m52}, p < 0.001) (Figure 3). Moreover, wild-type SSR membranes were significantly more convoluted than *dlg* mutants (index of convolution = 36.3 ± 12.7 in wild type versus 11.0 ± 5.9 in *dlg*^{m52} and 16.3 ± 4.0 in *dlg*^{v59}, p < 0.001). In contrast, the density of SSR membranes was similar in both wild type and *dlg*^{v59} mutants, although it was slightly reduced (p< 0.01) in *dlg*^{m52}(Figure 3). In the *dlg*^{m52}*; post-dlg* strain, the SSR cross-sectional length, SSR thickness, and index of convolution were similar to wild type (63.8 ± 5.0 μm^{-1}, 0.28 ± 0.02 μm^{-1}, and 30.7 ± 3.2, respectively; Figure 3). However, the density of SSR membranes was about 35% lower than wild type (13.6 ± 1.8 layers/μm versus 8.8 ± 2.0 layers/μm), suggesting an incomplete rescue (Figure 3). A similar, although weaker, rescue effect was observed when BG57 was used to drive *dlg* in the postsynaptic cell.

Overexpression of *dlg* Results in an Overdeveloped SSR

The above results demonstrate that providing DLG to the postsynaptic cell is enough to restore substantially the structural properties of *dlg* mutant SSR. These observations support the model that suggests that *dlg* regulates or determines the size of the SSR. To test further this hypothesis, we increased DLG levels in wild-type postsynaptic muscles. This was accomplished by generating female flies with *UAS-dlg* in the first and second chromosomes and crossing them to the BG487 *Gal-4* line. In theory, males from this progeny (UAS-*dlg*/Y; UAS-*dlg*/BG487) should have three extra copies of *dlg*, assuming dosage compensation in the male X chromosome (Belote and Lucchesi, 1980). However, dosage compensation has not been demonstrated for transgenes.

The results from these experiments are shown in Figure 4 at the light microscopical level and in Figures 2 and 3 at the EM level. At the light microscopical level, DLG immunoreactivity around Type I boutons with extra postsynaptic DLG was clearly more extensive than in wild type (compare Figures 4A and 4B), resulting in a thicker immunoreactive area around Type I_b boutons. This was also observed at Type I_s boutons, which normally have a thinner SSR and stain lightly with DLG antibodies (Figure 4; Lahey et al., 1994). This more extensive DLG immunoreactivity did not seem to be simply the result of an increase in the intensity of the label, but rather of an increase in the area around Type I boutons that stained with anti-DLG antibodies. This was confirmed by the ultrastructural analysis (see Figure 2C and Figure 3).

At the EM level, the SSR at Type I_b boutons in larvae with postsynaptic DLG overexpression appeared more extensive than in wild type, expanding over a larger area of the postsynaptic junctional region (see Figure 3C). The normalized cross-sectional SSR length (88.4 ± 9.4 μm^{-1}) and SSR thickness (0.38 ± 0.06 μm^{-1}) in these larvae were significantly larger (p < 0.01) than in wild type (about 39% and 36% change, respectively; see Figure 3). In contrast, both the SSR density and index of convolution were similar to wild type. Similar results were obtained in a strain with only two extra *dlg* copies (see Figure 3). These results, together with the results in the mutants, provide strong evidence that the levels of postsynaptic DLG regulate or determine SSR size.

Synaptic Transmission Is Also Altered in *dlg* Mutants

The previous experiments, as well as the studies of Lahey et al. (1994) demonstrated that changes in *dlg* levels have profound effects on the structure of the postsynaptic surface at Type I boutons. We next investigated if manipulation of *dlg* levels affected synaptic function.

Nerve-evoked and spontaneous synaptic currents were examined at muscles 6 and 7 using two electrode voltage clamp. The segmental nerve that innervates each hemisegment was stimulated at 0.1 Hz to elicit EJCs (Figure 5A). Muscles 6 and 7 are innervated by two motorneurons, RP3 and 6/7b, whose boutons innervate both muscle fibers (reviewed by Keshishian and Chiba, 1993). As shown by Kurdyak et al. (1995), by simultaneously recording from the muscle and from single Type I_b and Type I_s boutons, these two motorneurons can be distinguished by their stimulus threshold and EJC amplitude. Type I_b boutons generally become activated at lower stimulation voltage and elicit an EJC with significantly smaller amplitude. In agreement with these studies, we found that in about 80% of the muscle fibers, we could distinguish two classes of EJCs with different amplitudes by adjusting the stimulus voltage. For the following analysis, we only used muscle fibers in which the two populations of EJCs could be clearly distinguished.

In normal larvae in 1.5 mM Ca^{2+}, the EJC elicited by lower stimulation voltage, which corresponds to the activation of Type I_b boutons (Kurdyak et al., 1995), had an amplitude of 48.9 ± 4.6 nA (8 samples, 15 muscle fibers; Figures 5A and 5B; Table 2). At suprathreshold stimulation voltages, an EJC of 84.2 ± 3.8 nA (8 samples, 15 muscle fibers), almost certainly corresponding to a compound EJC elicited by the activation of both Type I_b and Type I_s, could be observed (Figures 5A and 5B). The decay time constant, assuming a single exponential model, was not significantly different in both classes of EJCs (8.9 ± 0.9 ms for Type I_b and 9.8 ± 0.6 ms for the compound EJC; Table 2).

In *dlg* mutants, two populations of EJCs that differ in amplitude and stimulation threshold could also be observed in most preparations. However, mutations in *dlg* might affect stimulus threshold; if so, our methodology would not be able to distinguish which of the bouton types is responsible for each EJC class. We will refer to these two EJC classes as the “low” and “supra” threshold EJCs. The amplitude of both EJC types was dramatically increased in the two *dlg* alleles, dlg^{m52} and dlg^{v59}. The amplitude of the low threshold EJC was 103.1 ± 3.6 nA in dlg^{v59}/Df (nine samples, ten muscle fibers) and 96.9 ± 4.4 nA in dlg^{m52}/Df (five samples, eight muscle fibers), 101% and 98% larger than in controls ($p < 0.0005$). Similarly, the amplitude of the suprathresh-old EJC was 154.6 ± 5.7 nA in dlg^{v59}/Df (nine samples, ten muscle fibers) and 161.7 ± 4.6 nA in dlg^{m52}/Df (five samples, eight muscle fibers), 84% and 92% larger than in control ($p < 0.0005$); Figures 5A and 5B). No significant change in the decay time constants was observed in the mutants (see Table 1).

The changes in EJC amplitude in the mutants could be due to presynaptic or postsynaptic defects (or both). At the presynaptic level, an increase in EJC amplitude could be the result of, for example, an increased number of vesicles released (quantal content) or of an increase in the amount of glutamate released by each vesicle. At the postsynaptic level, an increase in

EJC amplitude could be the result of a change in the passive properties of the membrane, of a change in glutamate receptor properties, or of a change in the distribution of receptors.

Capacitance and input resistance were calculated from the capacitive component and the leakage current during a 50 ms, 20 mV voltage step (from −80 to −60 mV). The specific membrane capacitance (Cs) and the specific resistivity (R_s) were calculated using measurements of muscle membrane surface (see Experimental Procedures). Measurement of 24 wild-type, 20 *dlg*^{v59}/ Df, and 16 *dlg*^{m52}*/Df* fibers showed that there was no significant change in R_s and C_s between wild-type and *dlg* mutant fibers (Table 2). Therefore, the increase in EJC amplitude observed in *dlg* mutants is not due to changes in passive properties of the muscle membrane.

dlg Mutants Have Increased Neurotransmitter Release

The spontaneous Ca^{2+}-independent release events (miniature EJCs) in each genotype were then determined. A postsynaptic change in glutamate receptor properties or number, or a change in the amount of glutamate released by each vesicle, should result in altered miniature EJC amplitude. Examination of a large number of miniature EJCs (17,942 in six wild-type preparations; 16,923 in five *dlg*^{v59}*/Df* preparations; 21,977 in five *dlg*^{m52}*/Df* preparations) revealed a unimodal distribution in each genotype (Figures 5C-5F). The mean quantal size was 0.40 ± 0.06 nA in wild type, 0.47 ± 0.01 nA in *dlg*^{v59}*/Df*, and 0.48 ± 0.02 nA in *dlg*^{m52}*/Df* (Table 2). There was a small but statistically insignificant increase in the miniature EJC amplitude in the mutants.

This result suggested that the change in EJC amplitude observed in *dlg* mutants was the result of a presynaptic defect rather than of a change in postsynaptic properties. This result was surprising, because the most dramatic morphological defect that we have observed in the mutants is postsynaptic. To confirm the hypothesis that *dlg* affected a presynaptic mechanism, we estimated the quantal content by stimulating the nerves at low Ca^{2+} concentration (0.4–0.6 M), using a suprathresh-old stimulation voltage, and dividing the EJC amplitude by the miniature EJC amplitude. We found that there was a 2- to 3-fold increase in quantal content, without significant changes in the Ca^{2+} dependency of the response (Figure 6D). This is consistent with our model that suggests that neurotransmitter release is increased in the mutant.

A presynaptic mechanism to explain the mutant defect in EJC amplitude was also supported by increasing DLG levels in motorneurons or muscles in *dlg* mutants. For these experiments, we used the *Gal-4* strain BG487 for muscle expression and the strain *sca-Gal-4* for motorneuron expression. The strain *sca-Gal-4* carries a *Gal-4* gene fused to the promoter of the neurogenic gene *scabrous* (Mlodzik et al., 1990). Transgenic flies containing the *sca-Gal-4* element drive Gal-4 expression in several embryonic ectodermal tissues, such as a subset of epithelial cells, sensory neurons (Mlodzik et al., 1990), and central neurons including motorneurons. This expression pattern persists during the first instar, but becomes dimmer in epithelial cells. At the body wall muscles, however, anti-βgal and anti-DLG immuno-reactivity is observed at Type I boutons in *sca-Gal-4*/ UAS-*LacZ* and *dlg/Df; sca-Gal-4*/UAS-*dlg* (*dlg; pre-dlg*) respectively, up to late first instar stage (Figures 7C and 7D).

No change in the increased EJC amplitude was observed in *dlg^{m52}; post-dlg* (see Figures 5A and 5B). The EJC amplitude at 1.5 mM Ca^{2+} in these larvae was 90.3 ± 1.4 nA for the low threshold EJC and 159.6 ± 5.9 nA for the suprathreshold (compound) EJC (six samples, ten muscle fibers). Therefore, the increase in postsynaptic DLG levels in *dlg^{m52}; post-dlg* does not rescue the EJC mutant phenotype. In contrast, increases in DLG levels in the presynaptic cell restored almost completely the mutant phenotype (seven samples, ten fibers; see Figures 5A and 5B). The low threshold EJC amplitude in *dlg^{m52}; pre-dlg* was 58.6 ± 8.6 nA, which is indistinguishable from the low threshold wild-type EJC, and the high threshold EJC was 104.4 ± 10.4 nA, significantly larger than the wild-type compound EJC ($p < 0.025$), but significantly lower than in *dlg^{m52}/Df* ($p < 0.0005$). These results, taken together with the measurements of quantal content and quantal size, strongly suggest that the alteration of EJC amplitude in *dlg* mutants is the result of a presynaptic defect.

Depression and facilitation of synaptic signals are believed to be the result of presynaptic properties. Depression may result from limitation of energy supply (Atwood and Nguyen, 1995) or from a decrease in the releasable pool of synaptic vesicles owing to high frequency stimulation. Facilitation is thought to be the result of residual Ca^{2+} accumulation in the presynaptic terminal when temporally close stimuli are elicited (Kamiya and Zucker, 1994). Depression was elicited in wild-type and *dlg* mutant motor endings by suprathreshold stimulation at 10 Hz in 1.5 mM Ca^{2+}. Under these conditions, EJCs rapidly decreased in amplitude in both wild type and mutants (see Figure 6A). We found no significant difference in the depression index (amplitude of tenth EJC/amplitude of the first EJC) between wild type and *dlg* mutants (0.72 ± 0.13 in wild type, 0.61 ± 0.08 in *dlg^{v59}*, and 0.61 ± 0.06 in *dlg^{m52}*) (see Figure 6C). Stimulation at 5–10 Hz in 0.6 mM Ca^{2+}, in contrast, resulted in an increased EJC amplitude with each subsequent pulse in wild type and *dlg* mutant (see Figure 6B). As in the case of depression, no significant difference in facilitation index (amplitude of third EJC/amplitude of first EJC) was found between wild type and mutants (see Figure 6C).

Presynaptic DLG Expression Is Sufficient to Rescue the Postsynaptic Morphological SSR Phenotype

The presynaptic nature of the physiological defect observed in *dlg* mutants suggested that *dlg* functions in both the pre- and postsynaptic cell. This observation is consistent with our previous immunoEM studies, which indicate that DLG is expressed in both the pre- and postsynaptic cell (Lahey et al., 1994). Moreover, we have recently shown that during late embryonic stages, DLG is concentrated in the growth cone and is not observed postsynaptically until the larval stages (Guan et al., 1996). These observations raised the possibility that presynaptic DLG may also influence the structure of the postsynaptic SSR.

To address this possibility, we examined the effects of driving *dlg* expression in the presynaptic cell, and we observed the morphology of the SSR in *dlg* mutants, using the *sca-Gal-4* strain. At the light microscopical level, *dlg^{m52}; pre-dlg* Type I boutons resembled the wild type (data not shown). At the EM level, a rescue of the SSR phenotype was readily apparent (see Figure 2E and Figure 3). In *dlg^{m52};pre-dlg*, the SSR was very extensive, although it appeared somewhat less convoluted than in the wild type. Morphometric analysis

revealed that both the cross-sectional SSR length (89.0 ± 15.5 μm^{-1}) and the SSR thickness (0.46 ± 0.13 μm^{-1}) were significantly larger than in both *dlg* mutants and wild type. Both the index of convolution and SSR density were substantially smaller than in wild type ($p < 0.001$; 22.9 ± 2.6 μm^{-1} and 7.8 ± 0.53 layers/μm, respectively). However, the index of convolution was significantly larger than in *dlg* mutants ($p < 0.001$). These results were surprising, because they suggested that properties of the postsynaptic junction could be regulated by interactions with the presynaptic cells.

We confirmed these results with a second *Gal-4* strain, BG380. In BG380, Gal-4 expression is restricted to Type I motorneurons, a few epidermal cell patches, and tracheal cells along the major tracheal branches. In contrast to *sca-Gal-4*, BG380 Gal-4 expression in motorneurons starts by the end on the first instar stage, and no expression is seen during the embryonic stage. Figure 7A shows the expression of βgal in Type I boutons of BG380/ UAS– *LacZ*, and Figure 7B the expression of DLG in these boutons in dlg^{m52}*/Df; UAS-dlg*/ BG380. As with the *sca-Gal-4* strain, we found that targeting DLG to Type I boutons was enough to completely rescue most SSR alterations (see Figure 3). These results, taken together with the electrophysiological results, suggest that both pre- and postsynaptic mechanisms contribute to the final architecture of the SSR.

Discussion

Both Pre- and Postsynaptic DLG Levels Influence SSR Development

Our former studies demonstrated that *dlg* was required for normal development of Type I_b bouton SSR (Lahey et al., 1994). In the presence of abnormal DLG protein, the SSR formed but developed slowly, remaining less extensive and less complex than normal (Lahey et al., 1994; Guan et al., 1996). This phenotype represents a hypomorphic phenotype, since the mutant alleles used are not null, but rather generate abnormal forms of the DLG protein. In dlg^{v59} most of the guanylate kinase is deleted, but PDZs and SH3 domains are normal (Woods and Bryant, 1991). In dlg^{m52}, PDZ1 and 2 are intact, but the rest of the protein is deleted (Woods et al., 1996). Moreover, maternal DLG may provide some form of phenotype protection. Nonetheless, the abnormal development of the SSR during target muscle growth suggests that *dlg* is required for the regulation of SSR surface. In this paper, we tested this hypothesis by selectively modifying DLG levels in a subset of postsynaptic muscle cells and in motorneurons, using the *Gal-4* enhancer trap system (Brand and Perrimon, 1993). In addition, we investigated the physiological consequences of altering DLG levels at pre- and postsynaptic sites.

When *dlg* mutant muscles were provided with a normal *dlg* gene (driven by Gal-4), DLG protein became clustered around Type I boutons as it does in wild type. This normal targeting of DLG to only Type I boutons was evident even in a muscle fiber that is innervated by an additional bouton type, Type II. This observation indicates that the *UAS-dlg* insert behaves like the endogenous *dlg* regarding protein localization. Targeting DLG to the postsynaptic cell was sufficient to rescue substantially the mutant phenotype at the Type I_b bouton postsynaptic region, and the SSR developed to nearly wild-type levels. Moreover, when we overexpressed *dlg* in wild-type larvae, the SSR became overdeveloped, having a larger surface than normal. These results, together with the observation that in *dlg* mutants

the SSR is poorly developed, strongly suggest that *dlg* functions in the postsynaptic cell to regulate the size of the post-synaptic surface.

Even though increases in postsynaptic DLG were sufficient to modify the SSR size, we demonstrated that there was not an absolute requirement of postsynaptic DLG for normal development of the SSR; targeting DLG to the presynaptic cell in a mutant background was also enough to rescue substantially the abnormalities at the SSR. This result has very interesting implications. First, it indicates that DLG protein does not determine SSR size but rather that it regulates its development, since in the absence of normal postsynaptic DLG, but, in the presence of presynaptic DLG, the SSR can still develop to nearly wild-type levels. Second, it suggests that the structure of postsynaptic specializations can, at least in part, be regulated by the presynaptic cell.

While many aspects of postsynaptic development in flies occur in an autonomous fashion, others require input from the presynaptic cell. For example, muscle development and the localization of junctional proteins, such as connectin, occur independently of muscle innervation (Broadie and Bate, 1993a, 1993b). In contrast, other processes, such as the clustering of glutamate receptors (GluR) or the up-regulation of these receptors, require innervation by the presynaptic cell (Broadie and Bate, 1993b). Though a GluR clustering protein is required in the postsynaptic cell, the signal to activate its synthesis or its conversion into a functional state requires a presynaptic signaling mechanism. Similarly, at the vertebrate neuromuscular junction, the nerve-derived extracellular matrix protein, agrin, is targeted to and released by the presynaptic ending, activating the mechanisms of acetylcholine receptor (AChR)clustering at the postsynaptic muscle (Fallon and Hall, 1994). Once this signaling mechanism is activated, the protein rapsyn, which interacts directly with AChR, induces their clustering at the postsynaptic junctional region (Apel and Merlie, 1995).

A comparable mechanism may be operating at the Drosophila larval neuromuscular junction. In wild type, DLG is associated with both pre- and postsynaptic membranes (Lahey et al., 1994). However, DLG is observed in the presynaptic cell prior to its expression in the postsynaptic cell (Guan et al., 1996). The expression of DLG in the presynaptic cell may target ion channels and other proteins to the presynaptic terminal and activate the release of an agrin-like molecule, which induces the synthesis of rapsyn-like synapse-organizing proteins, such as DLG in the postsynaptic cell. These post-synaptic proteins would cluster ion channels and receptors and gather structural and membrane components to build the postsynaptic apparatus. When normal DLG is expressed only in the presynaptic cell, the synthesis of synapse-organizing proteins in the postsynaptic cell would be induced, and many aspects of postsynaptic assembly would be normal. However, because DLG protein is abnormal in the postsynaptic cell, some properties of the postsynaptic apparatus would be altered. Similarly, the presence of normal DLG in the postsynaptic cell alone would allow only partial organization of the postsynaptic apparatus. In this regard, it is interesting to note that SSR rescue was more complete when DLG was targeted to the presynaptic cell.

An alternative possibility to explain the SSR rescue by presynaptic DLG is that the *Gal-4* strains used to target DLG to the presynaptic cell also produce low levels of Gal-4 in the postsynaptic cell. Although this possibility can not be completely ruled out, no βgal-immunoreactive signal was observed in the muscle cells or any mesodermally derived cell throughout development, even though the anti-βgal antibody used produces virtually no background signal. The possibility that DLG may be transferred from the presynaptic terminal to the muscle would, at first, seem to be an attractive possibility. However, based on the deduced DLG amino acid sequence and on the deduced amino acid sequence of any of the MAGUKs described so far, there is no evidence to indicate that DLG is a secreted protein.

Presynaptic DLG Also Affects Neurotransmitter Release

Standard voltage clamp techniques were used to analyze synaptic currents at the ventral longitudinal muscle fibers 6 and 7. Both of these muscle fibers are innervated by Type I_b and Type I_s boutons provided by two motorneurons, RP3 and 6/7b (Keshishian and Chiba, 1993). Type I_b excitatory junctional currents have been demonstrated to have a lower stimulus threshold and a smaller EJC amplitude. Type I_s synaptic currents, on the other hand, cannot be stimulated in isolation but are recruited by higher stimulation voltages in conjunction with Type I_b EJCs, forming a compound EJC (Kurdyak et al., 1995). Consistent with this report, we distinguished two populations of EJCs with different amplitudes and stimulation threshold in both wild type and *dlg* mutants. Because in *dlg* mutants the stimulation threshold for each motorneuron may change, the identity of the lower threshold EJC as Type I_b EJC cannot be determined with certainty using our methodology. We therefore referred to both classes of EJCs as the “low” and “high” threshold EJC. Since suprathreshold stimulation voltages were used to generate the high threshold EJC, we are certain that both motorneurons were recruited.

A dramatic increase (80%-100%) in the amplitude of high and low threshold EJCs was observed in both *dlg* alleles used. The kinetic properties of EJCs in the mutants, however, were not altered. The change in EJC amplitude was not due to an alteration in membrane passive properties, as indicated by our measurements of specific membrane resistivity and capacitance.

To determine if the increase in EJC amplitude was due to a pre- or postsynaptic defect, we investigated the size distribution of miniature EJCs. A miniature EJC is believed to result from spontaneous (not evoked) Ca^{2+}-independent neurotransmitter release from the fusion of a single synaptic vesicle to the presynaptic membrane (Del Castillo and Katz, 1954). An invariant miniature EJC amplitude (quantal size) accompanied by a change in EJC amplitude has classically been interpreted as a change in presynaptic release properties, whereas a change in quantal size is likely to result from a change in the properties of postsynaptic receptors (e.g., Dudel and Kuffler, 1961; Zhong and Shanley, 1995). In *dlg* mutant muscles, no alterations in miniature EJC size were observed. We therefore examined the possibility that the enlarged EJC amplitude in *dlg* mutants was caused by an increase in the number of vesicles released during each stimulus (quantal content).

Our hypothesis was confirmed by two independent methods: first, by estimating the quantal content from the ratio of mean EJC amplitude to mean miniature EJC amplitude; second, by selectively targeting *dlg* expression to either the pre- or the postsynaptic cell in *dlg* mutants.

The first method (mean EJC amplitude/mean miniature EJC amplitude) revealed about a 2- to 3-fold increase in quantal content in *dlg* mutants. Convincing evidence of a defect in synaptic transmission in the mutants was also obtained by selectively targeting DLG to *dlg* mutant pre- or postsynaptic cells. *dlg* expression in only the presynaptic cell was sufficient to rescue almost completely the defect on synaptic currents observed in *dlg* mutants. In contrast, DLG targeting to the postsynaptic cell, though it partially rescued the structural alterations, did not rescue the alterations in EJC amplitude. This result is consistent with our hypothesis that the alterations in synaptic transmission in the mutants are presynaptic. However, besides a small decrease in vesicle density in one of the *dlg* mutant alleles, no ultrastructural alterations in presynaptic boutons was found.

In mammalian systems, several *dlg* homologs, such as PSD-95/SAP-90, SAP-97, and chapsyn, are expressed at pre- or postsynaptic sites (or both) (reviewed by Garner and Kindler, 1996). Recent studies also show that PSD-95/SAP-90 interacts directly with channels such as the NMDA receptor and a Shaker-like channel (Kim et al., 1995; Kornau et al., 1995). The binding between this channel and PSD-95/SAP-90 occurs between an amino acid motif (tSXV) present at the carboxyl end of these channels, and the PDZ-2 domain of PSD-95/ SAP-90. This motif is present in both mammalian and fly Shaker channels, the NMDA receptor, a number of glutamate receptor channels, sodium channels, other receptors and cell adhesion molecules such as Fasciclin II, and the nerve growth factor receptor (Kornau et al., 1995). These studies also demonstrate the ability of the PSD-95/SAP-90 protein to cluster Shaker-type channels and NMDA receptors (Kim et al., 1995, 1996; Kim and Sheng, 1996), suggesting that MAGUKs may be involved in the organization of pre- or postsynaptic specializations (or both).

Similarly, DLG is localized at Type I bouton pre- and postsynaptic sites, and proteins with a tSXV motif, such as Shaker channels and Fasciclin II, are also expressed at these sites (Cho et al., 1992; Tejedor et al., submitted). Moreover, alterations of DLG levels at each of these sites lead to synaptic defects. For example, alterations in transmitter release could be due to abnormal localization of Shaker channels at the presynaptic bouton, which would result in a prolonged repolarization of action potentials in the terminal, a larger influx of Ca^{2+} through voltage-dependent Ca^{2+} channels, and increased neurotransmitter release. This is consistent with the observation that in *Shaker* mutants, in which I_A is abolished, action potentials are prolonged and neurotransmitter release is increased (Ganetzky and Wu, 1983). Similarly, altered postsynaptic structure may be due to abnormal clustering of postsynaptic proteins required for mature SSR formation.

In the CNS, DLG is expressed in the neuropil (Woods and Bryant, 1991). However, it is not clear whether all processes in the neuropil express DLG. At the larval neuromuscular junction, where synapses can be singly identifed, DLG is expressed at Type I synapses and no specific staining is observed at Type II endings. While immunoreactivity is observed at Type III boutons in muscle 12, this immunoreactivity is not decreased in any of the mutant

alleles examined, and therefore almost certainly represents cross-reactivity with another antigen at Type III boutons (Lahey et al., 1994). This synaptic specificity argues that DLG is not the only synapse-organizing protein, and that other DLG-like proteins must exist. In this regard, it is interesting that both pre-and postsynaptic structure is different in these three bouton types (Jia et al., 1993) and that each bouton type releases a different complement of neurotransmitters (Johansen et al., 1989; Gorczyca et al., 1993; Monastirioti et al., 1995). At the vertebrate nervous system, several MAGUKs, coded by different genes, are differentially expressed (reviewed by Garner and Kindler, 1996). For example, PSD-95 appears to be expressed at glutamatergic and GABAergic synapses at both pre- and postsynaptic sites, while SAP97 is preferentially found at presynaptic sites (Müller et al., 1995; reviewed by Garner and Kindler, 1996). This observation suggests that several MAGUKs may be involved in the organization of different aspects of the synapse and that the presence of different MAGUKs would allow synapse diversity. While *dlg* is the only MAGUK reported in the Drosophila CNS so far, others may remain to be discovered.

Role of *dlg* on the Development and Plasticity of Drosophila Neuromuscular Junctions

Neuromuscular junctions in Drosophila larvae are dynamic structures that are continuously changing. Both the number of active zones in the presynaptic cell as well as the size and complexity of the SSR increase as target muscles grow during larval development (Gorczyca et al., 1993; Jia et al., 1993; Guan et al., 1996). These changes suggest that at any stage of development there must be a mechanism to coordinate the level of neurotransmitter output with the number of postsynaptic receptors. This mechanism would ensure that, despite changes in target size and number of active zones, the motorneuron would be able to drive muscle contraction. The nature of this signaling mechanism is not known but may involve interactions between the pre-and postsynaptic membrane through adhesion molecules, release of retrograde and anterograde messages, synaptic activity, or a combination of these processes.

That changes in DLG levels in the presynaptic cells are enough to influence both neurotransmitter release and SSR development raises the possibility that levels of activity may be one mechanism by which postsynaptic structure is regulated. A change in neurotransmitter release levels, for example, may affect the local accumulation of DLG at the postsynaptic membrane, and therefore the number of postsynaptic receptors, channels, and cytoskeletal proteins that become clustered at the synapse. In this context, it is noteworthy that two classes of Type I boutons, Type I_b and Type I_s, that elicit EJCs with different amplitudes and that have a different SSR size innervate muscles 6 and 7 (Atwood et al., 1993; Jia et al., 1993; Lahey et al., 1994; Kurdyak et al., 1995). Type I_s, which shows a larger EJC amplitude than Type I_b, stains much lighter with anti-DLG antibodies and has a significantly smaller SSR (Jia et al., 1993; Lahey et al., 1994; Kurdyak et al., 1995). Interestingly, in *dlg* mutants, in which the SSR is significantly reduced, EJCs also have a much larger amplitude.

The possibility of an activity-dependent regulation of synapse structure has been investigated in flies using combinations of Shaker channel mutants (Budnik et al., 1990; Jia et al., 1993). These studies revealed that the number of synaptic boutons and neuromuscular

arborizations are increased in hyperexcitable mutant combinations that affect potassium channels (Budnik et al., 1990). At the ultrastructural level, certain aspects of presynaptic morphology are also affected, but no general postsynaptic defects have been observed (Jia et al., 1993). These results suggest that levels of activity alone may not be enough to change dramatically SSR development. An alternative possibility is that the postsynaptic cell may influence the neurotransmitter output by the presynaptic cell. This view, however, is not supported by our observations. We found that presynaptic *dlg* expression could rescue both the neurotransmitter release phenotype and the SSR structure. In contrast, postsynaptic *dlg* expression substantially rescued the SSR phenotype, but failed to restore the increased neurotransmitter release.

In conclusion, our studies show that *dlg* is one important synaptic component involved in determining both structural and functional properties of specific synapses. The identification of other genes that affect synapse structure and that may interact with *dlg* will enable us to determine the mechanisms by which the coordinated assembly of the pre- and postsynaptic apparatus is orchestrated during synapse development and plasticity.

Experimental Procedures

Fly Stocks and *Gal-4* Enhancer Trap Screen

Flies were maintained at 25°C in standard Drosophila medium. The enhancer trap lines BG487, BG57, and BG380 were generated in a screen for enhancer detector strains expressing Gal-4 in subsets of muscles and motorneurons. Single P[*Gal-4* w+] insertions were obtained by mobilizing a P[*Gal-4* w+] element in the second chromosome (obtained from Dr. K. Kaiser) using the jump starter strain P[ry + Δ2–3] (88B) as in Brand and Perrimon (1993). *Sca-Gal-4* was obtained from Dr. A. Chiba. *dlg* mutant stocks used in this study are described in Lahey et al. (1994). Canton-S was used as wild-type control strain.

Generation of UAS-*dlg* and Germline Transformation

A XhoI–BamHI fragment containing the complete *dlg-A* cDNA sequence (Woods and Bryant, 1991) was subcloned into the pUAST vector (Brand and Perrimon, 1993) to give rise to pUAS-*dlg*. Transgenic flies were generated by injecting 0.5 mg/ml pUAST-*dlg* and helper plasmid Δ2–3 purified in a Quiagen column into w^{118} embryos using standard methods (Spradling, 1986). The *dlg-A* cDNA corresponds to the largest of the two transcripts found during larval stages. The smaller transcript lacks the GUK domain, and our previous studies have shown that this domain is necessary for normal SSR development (Lahey et al., 1994).

Immunocytochemistry

Immunocytochemical methods were carried out as in Lahey et al. (1994). The following primary antibodies and dilutions were used: anti-DLG antibodies (Woods and Bryant, 1991), 1:250–1:500 dilution; anti-βgal polyclonal antibody (Cappel), 1:1000 dilution; goat or rabbit anti-HRP antiserum (Sigma), 1:400 dilution. Rhodamine-conjugated phalloidin (Molecular Probes) was used to stain muscle actin. Secondary antibodies (Jackson Laboratory or Cappel) were either conjugated to Texas red or fluorescein. All light microscopical images

were made on a BioRad MRC 600 confocal microscope attached to a Nikon inverted scope. Software programs NIH Image 1.57 and Photoshop 3.0 were used to analyze and construct images.

EM and Morphometric Analysis

Transmission EM was carried out as in Jia et al. (1993). Semiserial cross-sectional thin sections of muscles 6 and 7 (segment A2 or A3) were cut, and Type I_b boutons photographed. Within a bouton, only the largest diameter section, corresponding to the bouton midline, was analyzed. For morphometric analysis of the SSR, electron micrographs were printed at 30,000× , the SSR traced, scanned into a computer, and analyzed using NIH image 1.57. Four different measurements were performed as follows.

SSR Cross-Sectional Length—The length of each SSR membrane segment was determined using the “Analyze particles” function of NIH Image. The length of each segment was added to obtain the total cross-sectional SSR length. Both SSR cross-sectional length and thickness (see below) were normalized by the area of the presynaptic bouton. However, the differences between wild-type and mutant strains were similar, even without such normalization.

SSR Thickness—The distance between the presynaptic membrane and the distal-most SSR membrane was measured. Four different measurements at 90° angle from each other were performed for each bouton. The SSR thickness at each bouton was expressed as the average of the four measurements.

SSR Density—The number of membrane segments crossed by a line traced from the presynaptic membrane to the distal-most SSR membrane was determined by using the “plot profile” function of NIH Image. This number was then divided by the SSR thickness to calculate the number of layers per μm. Four measurements at 90° angle were performed per bouton.

Index of Convolution—Four 0.5 μm^2 SSR areas localized close to the presynaptic membrane, and at ~90° angle from each other, were selected. The average angle between the presynaptic membrane and each membrane segment was determined using the “Analyze particles” function of NIH image. The index of convolution was defined as the percentage of membrane segments that were between 45° and 135° with respect to the presynaptic membrane. This parameter estimated the deviation from concentricity of each SSR membrane layer (Lahey et al., 1994). Overall, three wild type (17 boutons), three dlg^{m52}/Df (22 boutons), three $dlgm^{52}$*; post-dlg* (18 boutons), two BG487/UAS-*dlg* (18 boutons), two UAS-*dlg;* BG487/UAS-*dlg* (19 boutons), and three dlg^{m52}*; pre-dlg* (15 boutons) were examined. SSR measurements were performed only in boutons where the limits of the SSR were clearly defined, were expressed as mean ± SEM, and compared by using the Student’s *t* test.

Electrophysiology

Electrophysiological recordings were performed in Stewart's saline (70 mM NaCl, 5 mM KCl, 1.5 mM $CaCl_2$, 20 mM $MgCl_2$, 10 mM $NaHCO_3$, 5 mM trehalose, 115 mM sucrose, 5 mM HEPES), as in Kurdyak et al. (1995). Because of the relatively high Mg^{2+} concentration in this saline, higher [Ca^{2+}] was required to elicit EJCs with amplitudes similar to those observed in other reports (e.g., Zhong and Shanley, 1995). Body wall muscles were dissected in Stewart's saline containing 0.4 mM $CaCl_2$, and individual muscle fibers visualized under a Zeiss inverted microscope using a 40x long distance objective. Muscles were impaled with 10–30 MΩ glass microelectrodes (about 10–12 MΩ for the current electrode and about 10–30 MΩ for the voltage electrode), pulled on a Flaming-Brown puller (Sutter Instruments), and filled with 2.5 M KCl. Two-electrode voltage clamp was performed using an Axoclamp 2A amplifier. The muscle membrane potential was held at −80 mV to prevent activation of voltage-gated channels and to provide a reference for comparison between different muscle fibers. Data was digitized using a Neurocorder Digitizing Unit (Neuro Data Instruments) and recorded on VCR tape for later analysis. Data was simultaneously recorded at low speed on a Gould chart recorder. Digitized data was transferred to a Macintosh IIci computer using a MacAdios Nubus board and analyzed using programs developed on site with Superscope 2.1 software.

To evoke EJCs, a single segmental nerve, which contains the axons that innervate muscles 6 and 7, was stimulated using a suction electrode (with a tip diameter of about 10 μm). The stimulus pulse duration was about 200–300 μs and its amplitude, between 5–15 V, was adjusted as desired to recruit one or two of the motor axons innervating muscles 6 and 7.

Passive membrane properties were determined as in Wu and Haugland (1985) and Haugland and Wu (1990). To measure membrane capacitance (Cm) and input resistance (Ri), muscle fibers were held at −80 mV and a 20 mV voltage step of 50 ms duration was given. The membrane capacitance was calculated by integrating the capacitive surge elicited in the first 2.5 ms after the voltage step. The input resistance was determined from the current difference during the voltage step. To estimate the specific capacitance and specific resistivity, body wall muscle preparations of wild type and *dlg* mutants were stained using FITC-conjugated phalloidin to stain muscle fibers. The surface area of muscles (S) was estimated assuming an elliptic muscle cross-section and by measuring muscle thickness (a), muscle length (L), and muscle width (b) at the confocal microscope, according to the equation $S=L2\pi\sqrt{(a^2+b^2)/2}$.

For experiments using multiple Ca^{2+} concentrations, preparations were superfused using a multiport manifold connected to each different solution. Complete exchange of solutions was achieved in about 30 s.

Acknowledgments

We wish to thank Drs. Eve Marder, Francisco Tejedor, James Trimarchi, and Andrew Hill for helpful comments on the manuscript, and Dr. Akira Chiba for providing the *sca-Gal4* strain. We also thank the reviewers for insightful comments and constructive criticism of the original version of this manuscript. We acknowledge the staff of the Electron Microscope and Image Facility at the University of Massachusetts for facilitating our ultrastructural and

confocal work. We are grateful to Dr. Peter Bryant, in whose lab some of this work was conducted. Supported by National Institutes of Health RO1 NS70032, K04 NS01786, and an Alfred P. Sloan fellowship to V. B.

References

Anderson MS, Halpern ME, Keshishian H. Identification of the neuropeptide transmitter proctolin in Drosophila larvae: characterization of fiber-specific neuromuscular endings. J. Neurosci. 1988; 8:242–255. [PubMed: 2892897]

Apel ED, Merlie JP. The assembly of the postsynaptic apparatus. Curr. Opin. Neurobiol. 1995; 5:62–67. [PubMed: 7773008]

Atwood HL, Kwan I. Synaptic development in the crayfish opener muscle. J. Neurobiol. 1976; 7:289–312. [PubMed: 956815]

Atwood HL, Nguyen PV. Neural adaptation incrayfish. Am. Zool. 1995; 35:28–36.

Atwood H, Govind CK, Wu C-F. Differential ultra-structure of synaptic terminals on ventral longitudinal abdominal muscles in Drosophila larvae. J. Neurobiol. 1993; 24:1008–1024. [PubMed: 8409966]

Belote JM, Lucchesi JC. Control of X chromosome transcription by the *maleless* gene in Drosophila. Nature. 1980; 285:573–575. [PubMed: 7402300]

Brand AH, Perrimon N. Targeted gene expression as a means of altering cell fates and generating dominant phenotypes. Development. 1993; 118:401–415. [PubMed: 8223268]

Broadie K, Bate M. Synaptogenesis in the Drosophila embryo: innervation directs receptor synthesis and localization. Nature. 1993a; 361:350–353. [PubMed: 8426654]

Broadie K, Bate M. Muscle development is independent of innervation during Drosophila embryogenesis. Development. 1993b; 119:533–543. [PubMed: 8287801]

Budnik V. Synapse maturation and structural plasticity at Drosophila neuromuscular junctions. Curr. Opin. Neurobiol. 1996; 6

Budnik V, Zhong Y, Wu C-F. Morphological plasticity of motor axon terminals in Drosophila mutant with altered excitability. J. Neurosci. 1990; 10:3754–3768. [PubMed: 1700086]

Cantera R, Nässel DR. Segmental peptidergic innervation of abdominal targets in larval and adult dipteran insects revealed with an antiserum against leucokinin I. Cell Tissue Res. 1992; 269:459–471. [PubMed: 1423512]

Cho K-O, Hunt CA, Kennedy MB. The rat brain postsynaptic density fraction contains a homolog of the Drosophila Disc-Large tumor suppressor protein. Neuron. 1992; 9:929–942. [PubMed: 1419001]

Del Castillo J, Katz B. Quantal components of the end-plate potential. J. Physiol. 1954; 124:560–573. [PubMed: 13175199]

Doyle DA, Lee A, Lewis J, Kim E, Sheng M, MacKinnon R. Crystal structures of a complexed and peptide-free membrane protein-binding domain: molecular basis of peptide recognition by PDZ. Cell. 1996; 85:1067–1076. [PubMed: 8674113]

Dudel J, Kuffler SW. Presynaptic inhibition at the crayfish neuromuscular junction. J. Physiol. 1961; 155:543–562. [PubMed: 13724752]

Fallon JR, Hall ZW. Building synapses: agrin and dystroglycan stick together. Trends Neurosci. 1994; 17:469–473. [PubMed: 7531888]

Ganetzky B, Wu C-F. Neurogenetic analysis of potassium currents in Drosophila: synergistic effects on neuromuscular transmission in double mutants. J. Neurogenet. 1983; 1:17–28. [PubMed: 6100303]

Garner C, Kindler S. Synaptic proteins and the assembly of the postsynaptic apparatus. Trends Cell Biol. 1996 in press.

Genisman Y, deToledo-Morrell F, Heller RE, Rossi M, Pars-hall RF. Structural synaptic correlate of long-term potentiation: formation of axospinous synapses with multiple, completely partitioned transmission zones. Hippocampus. 1993; 3:435–446. [PubMed: 8269035]

Goodman CS, Shatz CJ. Developmental mechanisms that generate precise patterns of neuronal connectivity. Neuron. 1993; 10:77–98.

Gorczyca MG, Augart C, Budnik V. Insulin-like receptor and insulin-like peptide are localized at neuromuscular junctions in Drosophila. J. Neurosci. 1993; 13:3692–3704. [PubMed: 8366341]

Guan B, Hartmann B, Kho Y-H, Gorczyca M, Budnik V. The Drosophila tumor suppressor gene, *dlg*, is involved in structural plasticity at a glutamatergic synapse. Curr. Biol. 1996; 6:695–706. [PubMed: 8793296]

Hall ZW, Sanes JR. Synaptic structure and development: the neuromuscular junction. Neuron. 1993; 10:99–121.

Jan LY, Jan YN. L-glutamate as an excitatory transmitter at the Drosophila larval neuromuscular junction. J. Physiol. 1976; 262:215–236. [PubMed: 186587]

Jia X, Gorczyca M, Budnik V. Ultrastructure of neuromuscular junctions in Drosophila: comparison of wild type and mutants with increased excitability. J. Neurobiol. 1993; 24:1025–1044. [PubMed: 8409967]

Johansen J, Halpern ME, Johansen KM, Keshishian H. Stereotypic morphology of glutamatergic synapses on identified muscle cells of Drosophila larvae. J. Neurosci. 1989; 9:710–725. [PubMed: 2563766]

Kamiya H, Zucker RS. Residual Ca^{2+} and short-term synaptic plasticity. Nature. 1994; 371:603–606. [PubMed: 7935792]

Keshishian H, Chiba A. Neuromuscular development in Drosophila: insights from single neurons and single genes. Trends Neurosci. 1993; 16:278–283. [PubMed: 7689772]

Kim E, Sheng M. Differential K^+ channel clustering activity of PSD-95 and SAP-97, two related membrane-associated putative guanylate kinases. Neuropharmacology. 1996 in press.

Kim E, Niethammer M, Rothschild A, Jan YN, Sheng M. Clustering of Shaker-type K^+ channels by interaction with a family of membrane-associated guanylate kinases. Nature. 1995; 378:85–88. [PubMed: 7477295]

Kim E, Cho K-O, Rothschild AR, Sheng M. Heteromultimerization and NMDA receptor clustering activity of chapsyn-110, a member of the PSD-95 family of synaptic proteins. Neuron. 1996; 17:103–113. [PubMed: 8755482]

Kistner U, Wenzel BM, Veh RW, Cases-Langhoff C, Garner AM, Appeltauer U, Voss B, Gundelfinger ED, Garner CC. SAP-90, a rat presynaptic protein related to the product of the Drosophila tumor suppressor gene *dlg-A* . J. Biol. Chem. 1993; 268:4580–4583. [PubMed: 7680343]

Kornau H-C, Schenker LT, Kennedy MB, Seeburg PH. Domain interaction between NMDA receptor subunits and the postsynaptic density protein PSD-95. Science. 1995; 269:1737–1740. [PubMed: 7569905]

Kurdyak P, Atwood HL, Stewart BA, Wu CF. Differential physiology and morphology of motor axons to ventral longitudinal muscles in larval Drosophila. J. Comp. Neurol. 1995; 348:1–10.

Lahey T, Gorczyca M, Jia X, Budnik V. The Drosophila tumor suppressor gene *dlg* is required for normal synaptic bouton structure. Neuron. 1994; 13:823–835. [PubMed: 7946331]

Lnenicka GA, Atwood HL. Age dependent long-term adaptation of crayfish phasic motor axon synapses to altered activity. J. Neurosci. 1985; 5:459–467. [PubMed: 3973678]

Mlodzik M, Baker NE, Rubbing GM. Isolation and expression of *scabrous*, a gene regulating neurogenesis in Drosophila. Genes Dev. 1990; 4:1848–1861. [PubMed: 2125959]

Monastirioti M, Gorczyca M, Rapus J, Eckert M, White K, Budnik V. Octopamine immunoreactivity in the fruit fly Drosophila melanogaster. J. Comp. Neurol. 1995; 356:275–287. [PubMed: 7629319]

Müller BM, Kistner U, Rudiger VW, Cases-Langhoff C, Becker B, Gundelfinger ED, Garner C. Molecular characterization and spatial distribution of SAP97, a novel presynaptic protein homologous to SAP90 and the *Drosophila* discs-large tumor suppressor protein. J. Neurosci. 1995; 15:2354–2366. [PubMed: 7891172]

Perrimon N. The maternal effect of *lethal(1) discs-large-1:* a recessive oncogene of Drosophila melanogaster. Dev. Biol. 1988; 127:392–407. [PubMed: 3132409]

Schmidt JT. Long-term potentiation and activity-dependent retinotopic sharpening in the regenerating retinotectal projection of goldfish: common sensitive period and sensitivity to NMDA blockers. J. Neurosci. 1990; 10:233–246. [PubMed: 2153773]

Spradling, AC. P element-mediated transformation. In: Robbers, DB., editor. Drosophila: A Practical Approach. Oxford, England: IRL Press; 1986. p. 175-197.

Weiler IJ, Hawrylak N, Greenough WT. Morphogenesis in memory formation: synaptic and cellular mechanisms. Behav. Brain Res. 1995; 66:1–6. [PubMed: 7755880]

Woods DF, Bryant PJ. The disc-large tumor suppressor gene of Drosophila encodes a guanylate kinase homolog localized at septate junctions. Cell. 1991; 66:451–464. [PubMed: 1651169]

Woods DF, Bryant PJ. ZO-1, DLGA and PSD-95/SAP-90: homologous proteins in tight, septate and synaptic cell junctions. Mech. Dev. 1993; 44:85–89. [PubMed: 8155583]

Woods DF, Hough C, Peel D, Callaini G, Bryant P. The Dlg protein is required for junction structure, cell polarity and proliferation control in *Drosophila* epithelia. J. Cell Biol. 1996 in press.

Wu C-F, Haugland FN. Voltage clamp analysis of membrane currents in larval muscle fibers of Drosophila: alteration of potassium currents in*shaker* mutants. J. Neurosci. 1985; 5:2626–2640. [PubMed: 2413182]

Zhong Y, Shanley J. Altered nerve terminal arborization and synaptic transmission in Drosophila mutants of cell adhesion molecule fasciclin I. J. Neurosci. 1995; 15:6679–6687. [PubMed: 7472428]

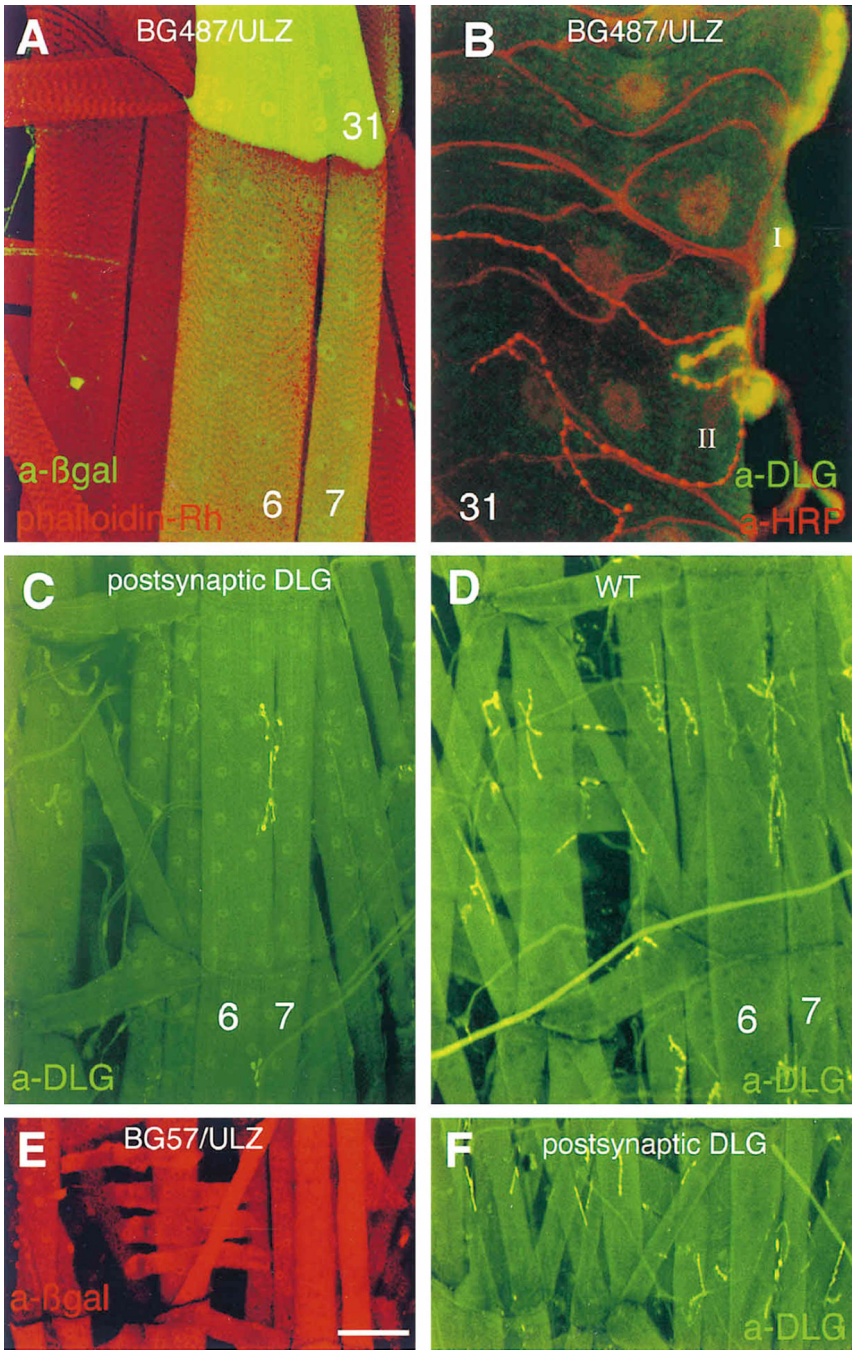

Figure 1. Targeted Expression of *dlg* in Postsynaptic Cells Results in DLG Localization to Type I Junctions

(A) Expression of Gal-4 in longitudinal muscles 6, 7, and 31 in the *P[Gal-4]* insertion line BG487 is detected by staining body wall muscles from progeny of the cross BG487 x UAS-*LacZ* with anti-βgal antibodies (green). All body wall muscles are double-labeled with rhodamine-conjugated phalloidin (red).

(B) View of muscle 31 in a dlg^{m52};*post-dlg* larva, in which the *Gal-4* strain BG487 has been used to target DLG expression in the muscle cell. This preparation has been double-labeled

with anti-DLG (green) and anti-HRP (red), a nervous system-specific antibody. Note that DLG is targeted only to Type I boutons in muscle 31, even though this muscle is innervated by both Type I and Type II endings.

(C) and (D) View of abdominal segment 2 in preparations stained with anti-DLG antibodies. DLG immunoreactivity at Type I boutons in muscles 6 and 7 in dlg^{m52}/Df; *post-dlg* (C). Note that in contrast to wild type (D), strong immunoreactivity is only observed at muscles 6 and 7 at Type I boutons.

(E) and (F) View of a late first instar body wall muscle segment. A BG57/UAS-*LacZ* preparation stained with anti-βgal antibodies (E), and a dlg^{m52}/Df; *UAS-dlg/+;* BG57/+ preparation stained with anti-DLG antibodies (F). These and subsequent light micrographs are confocal images, projected from a Z-series. Scale bars, 40 μm (A); 8 μm (B); 70 μm (C and D); and 20 μm (E and F).

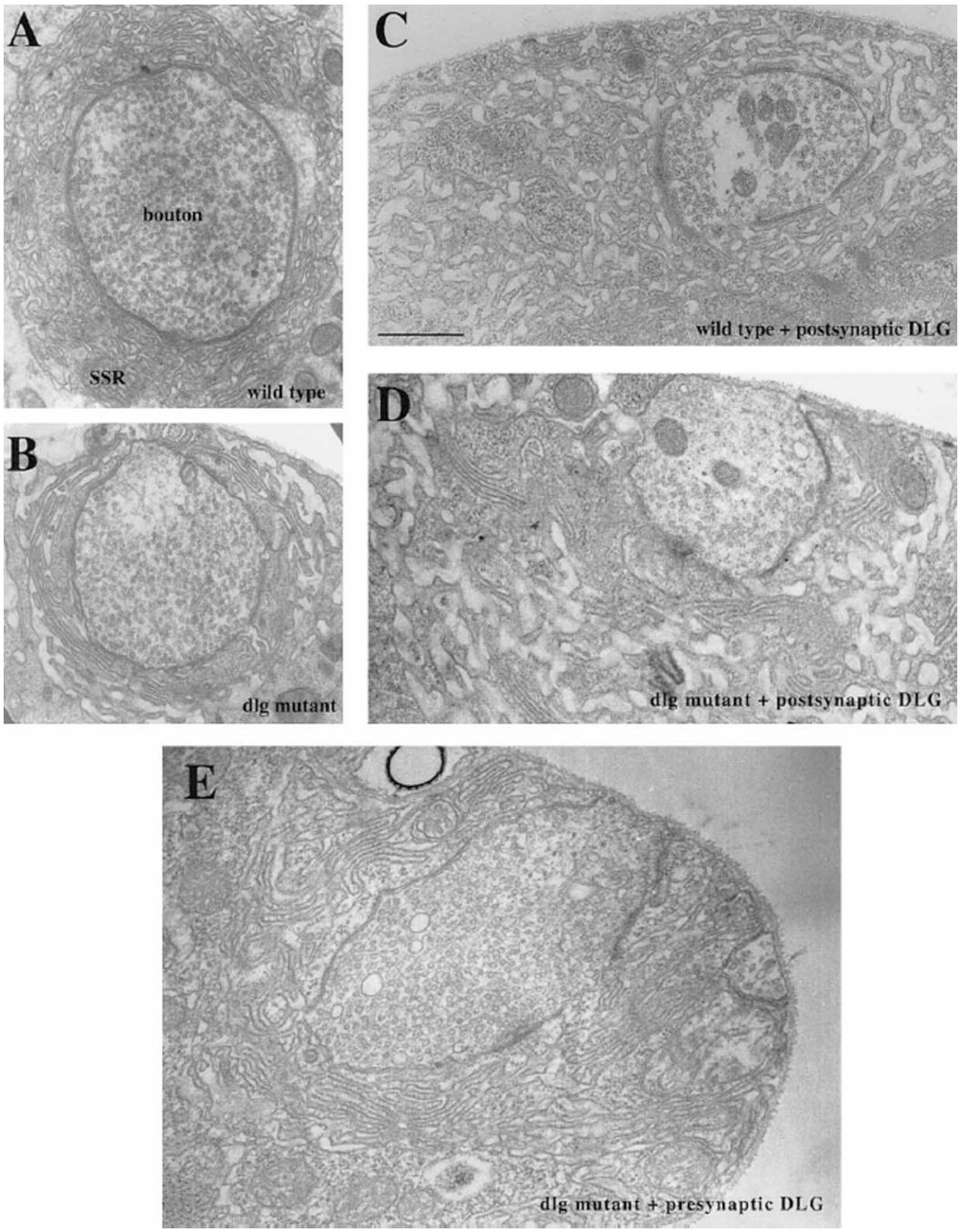

Figure 2. Regulation of SSR Size by *dlg*

(A) Electron micrograph of a Type I_b bouton in a wild-type larva, shows a normal SSR.

(B) In a dlg^{m52}/Df mutant larva, the SSR is underdeveloped.

(C) Postsynaptically driven *dlg (UAS-dlg*/ BG487) causes the SSR to appear overdeveloped.

(D) In a dlg^{m52}/Df mutant larva, *dlg* has been driven in the postsynaptic cell using BG487 (*dlg^{m52}; post-dlg*), and the mutant phenotype at the SSR has been partially rescued.

(E) Similarly, in a *dlg^{m52}; pre-dlg, dlg* has been driven in the presynaptic cells using *sca-Gal-4*, and the SSR appears normal. Scale bar, 0.8 μm.

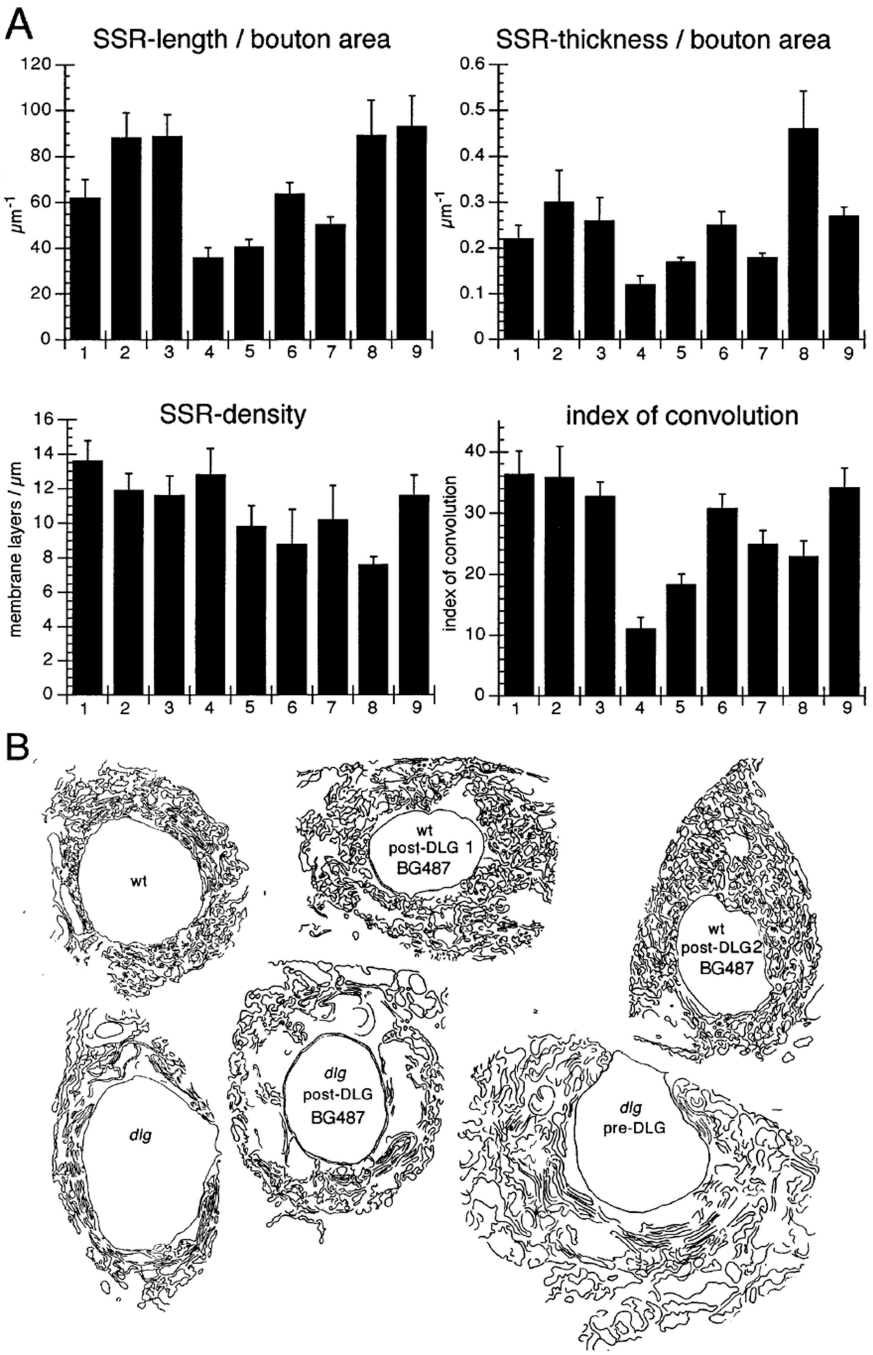

Figure 3. Morphometric Analysis of the SSR

(A) The normalized cross-sectional SSR length, normalized thickness, density, and index of convolution at Type I_b boutons are compared in nine genotypes as follows: in (1) wild type; (2) *post-dlg* (one copy UAS–*dlg* [UAS–*dlg*/BG487]); (3) *post-dlg* (two copies UAS–*dlg* [UAS–*dlg*/Y; UAS–*dlg*/BG487]); (4) dlg^{m52}/Df; (5) dlg^{v59}/Df; (6) *dlg–post-dlg* (dlg^{m52}/ Df; UAS–*dlg*/BG487); (7) *dlg–post-dlg* (dlg^{m52}/ Df; UAS–*dlg*/BG57); (8) *dlg–pre-dlg*(dlg^{v59}/- Df; *sca–Gal-4*/UAS–*dlg*); and (9) *dlg–pre-dlg* (dlg^{m52}/Df; UAS–*dlg*/BG380).

(B) Representative SSR tracing of some of the genotypes used for the analysis in (A) is diagrammed. The number of boutons used for the morphometric analysis is as follows: wild type: 12 boutons, wild type; *post-dlg* (one copy of UAS–*dlg)*): 12 boutons, wild type; *post-dlg* (two copies of UAS–*dlg*): 11 boutons; dlg^{m52}: 10 boutons; dlg^{v59}: 10 boutons; *dlg; post-dlg* (BG487): 18 boutons; *dlg; post-dlg* (BG57): 10 boutons; *dlg pre-dlg* (*sca–Gal-4*): 12 boutons; *dlg pre-dlg* (BG380): 10 boutons.

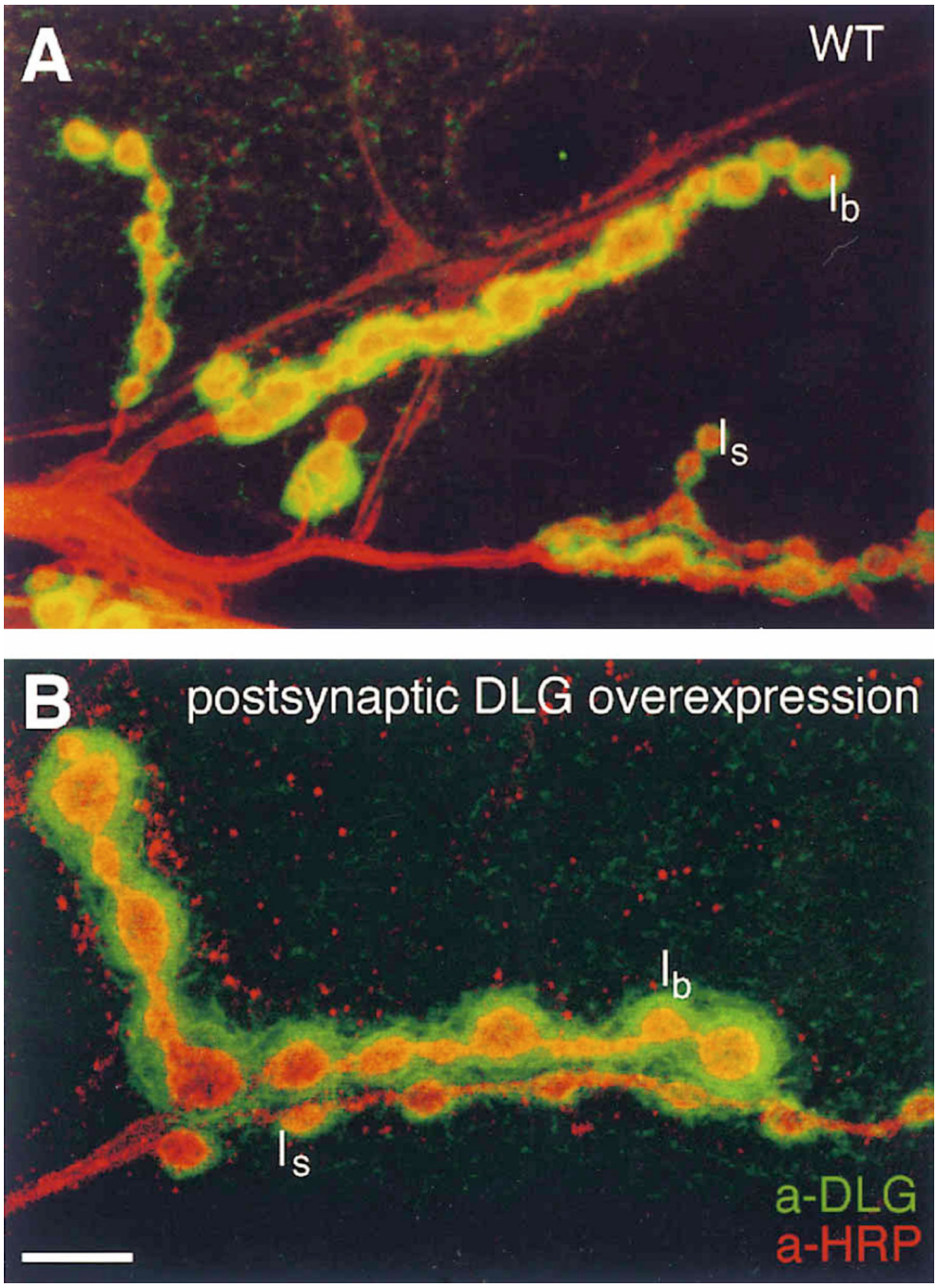

Figure 4. Postsynaptic *dlg* Overexpression Results in a Larger than Normal Immunoreactive Area around Type I Boutons

(A) and (B) Nerve endings in muscle 6 showing Type I_b and Type I_s boutons in preparations double-stained with anti-DLG (green) and anti-HRP (red) antibodies. Note how Type I_b boutons (B) in a larva with three extra *dlg* gene doses (UAS-*dlg*/Y; BG487/UAS-*dlg*) have very extensive DLG immunoreactivity compared to wild type (A). Scale bar, 10 μm.

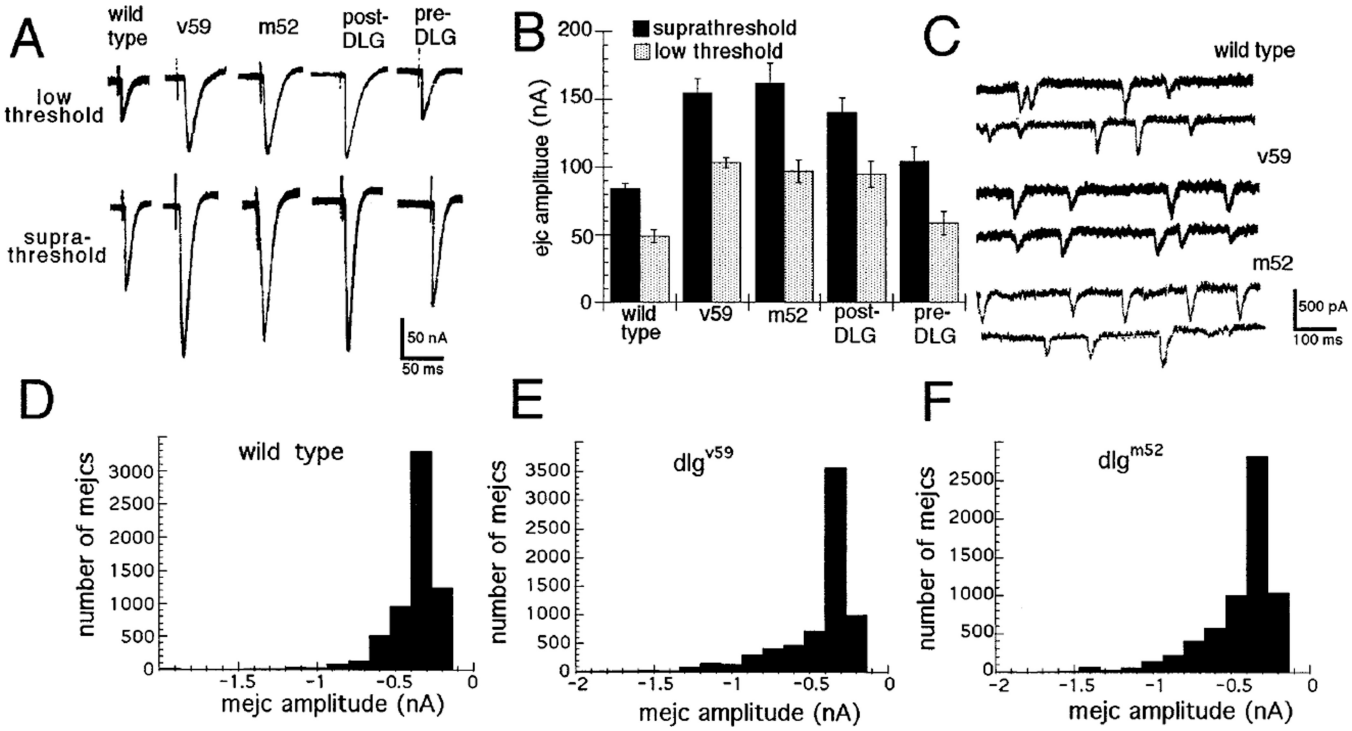

Figure 5. Evoked and Spontaneous Synaptic Currents Are Compared in Two *dlg* Mutant Alleles and in dlg^{m52}/Df with Pre- and Postsynaptic DLG Targeting

(A) Evoked currents were recorded in saline containing 1.5 mM Ca^{2+} in wild type, dlg^{v59}/Df mutants (v59), dlg^{m52}/Df mutants (m52), dlg^{m52}/ Df; *post-dlg*, in which *dlg* expression is driven postsynaptically (post-DLG), and dlg^{m52}/Df; UAS-*dlg/sca-Gal-4*, in which *dlg* expression is driven presynaptically (pre-DLG). Note that two classes of synaptic currents (low and suprathreshold EJCs) are observed in wild type and mutants and that their amplitude is increased in both *dlg* alleles. This abnormal phenotype is rescued in larvae with pre- but not postsynaptic expression.

(B) A histogram plot of the average low and suprathreshold EJC amplitudes (mean ± SEM).

(C) This panel shows examples of miniature EJCs in wild type, dlg^{v59}/Df, and dlg^{m52}/Df.

(D)-(F) Distribution of miniature EJC amplitudes is compared between wild type (D), dlg^{v59}/Df (E), and dlg^{m52}/Df (F).

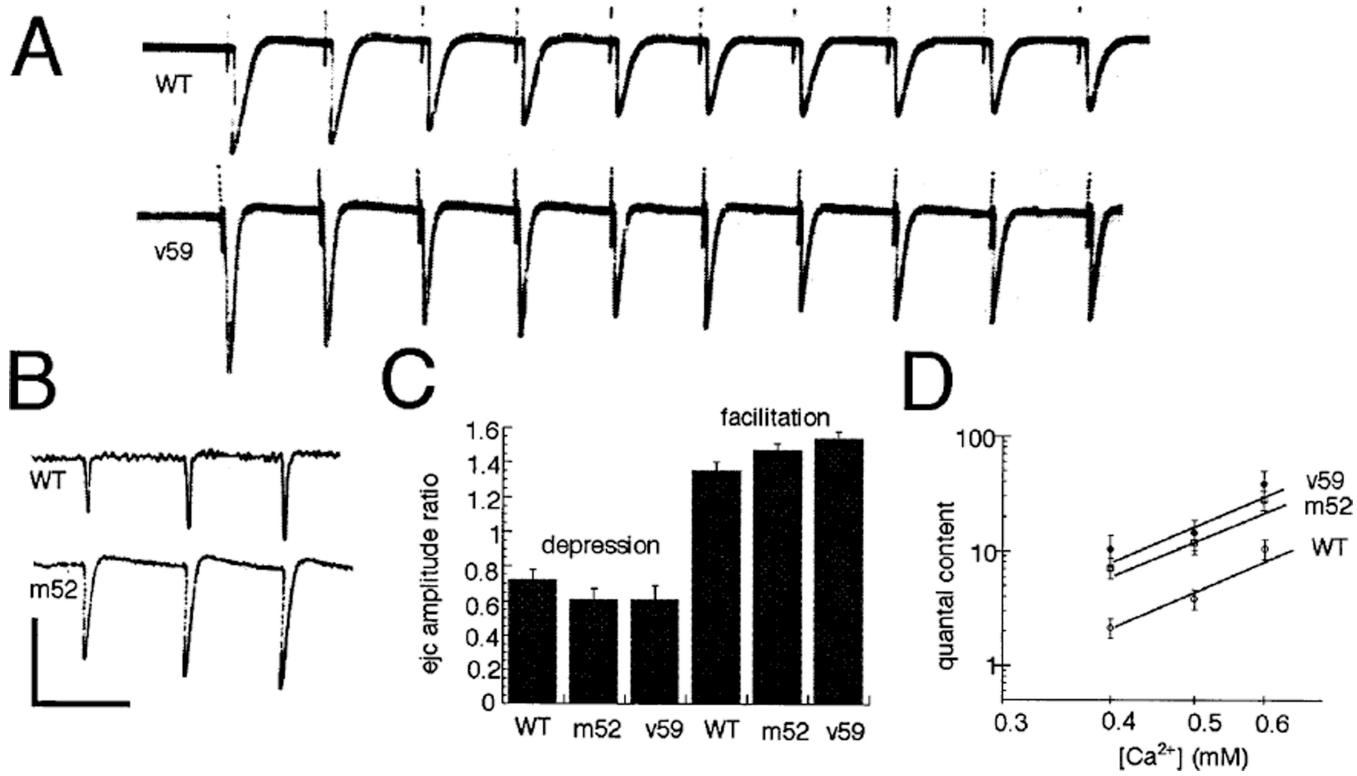

Figure 6. Short Term Plasticity of Wild-Type and *dlg* Mutant Synapses and Ca^{2+} Dependency of Quantal Content

(A) Train of EJCs in a wild type and dlg^{v59} mutant preparation stimulated at 10 Hz recorded in saline containing 1.5 mM Ca^{2+}. Note that both wild-type and mutant EJCs depress under these conditions.

(B) Train of EJCs in wild-type and dlg^{m52} preparations stimulated at 10 Hz recorded in saline containing 0.6 mM Ca^{2+}. Note that both wild-type and mutant EJCs facilitate.

(C) Histogram of the mean depression and facilitation index in wild-type and *dlg* mutant alleles.

(D) Double log plot of Ca^{2+} concentration versus quantal content demonstrates that mutant EJCs remain significantly larger than wild type at different Ca^{2+} concentrations and that the Ca^{2+} dependency of EJCs is unchanged. These results were obtained from at least four muscle fibers at each Ca^{2+} concentration and in each genotype. Calibration bars at the left corner correspond to 80 nA and 120 ms in (A), and to 20 nA and 100 ms in (B).

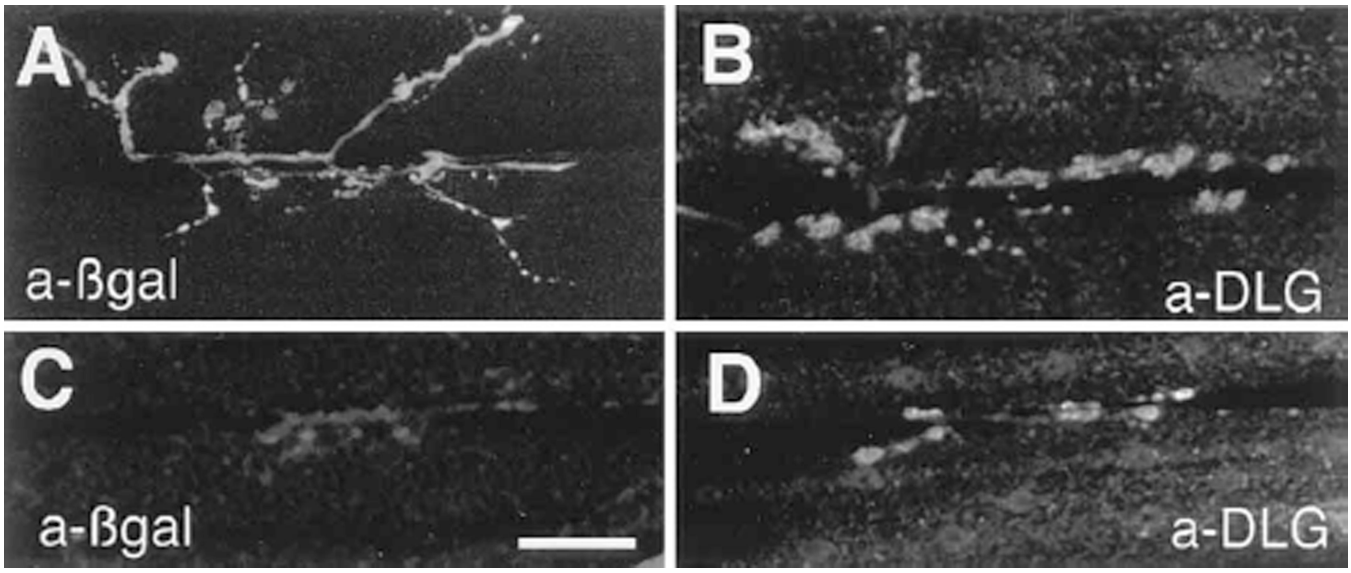

Figure 7. Targeting DLG to Presynaptic Endings

(A) and (B) Type I synaptic boutons in muscles 6 and 7 of a third instar BG380/UAS-*LacZ* preparation stained with anti-βgal antibodies (A), and of a third instar BG380/UAS– *dlg* sample stained with anti-DLG antibodies (B). Note that the boutons in (A) appear smaller than those in (B), probably owing to the differential localization of the antigens (cytoplasmic in the case of βgal, and membrane-associated in the case of DLG.

(C) and (D) Type I synaptic boutons in muscles 6 and 7 of a late first instar *sca-Gal-4*/U*AS-LacZ* stained with anti-βgal antibodies (C), and of a late first instar *sca-Gal-4*/U*AS-dlg* sample stained with anti-DLG antibodies (D). Scale bars, 20 μm (A and B); and 30 μm (C and D).

Table 1

Presynaptic Morphology of Wild Type and *dlg* Mutants

Anatomical Parameter	**Wild Type**	***dlg*^{m52}**	***dlg*^{v59}**
Vesicle density (Number of vesicles per 0.5 (μm^2)	39.3 ± 3.8	27.5 ± 3.5	51.3 ± 8.2
Number of active zones per cross-section	1.0 ± 0.24	1.4 ± 0.18	1.2 ± 0.25
Number of mitochondria	4.0 ± 0.45	2.9 ± 0.65	4.7 ± 0.9
Cross-sectional area	4.3 ± 0.51	4.1 ± 0.73	5.3 ± 0.82
Size of synaptic cleft (nm)	14.2 ± 0.38	13.9 ± 0.50	14.9 ± 0.53
Number of boutons analyzed	11	13	9

Table 2

Passive Membrane Properties, and EJC and Miniature EJC Values in Wild-Type and Mutant Strains with Different DLG Levels

Genotype	Peak EJC (Low Threshold) [nA]	Peak EJC (Supra-Trheshold) [nA]	τDecay (Type I_b) [ms]	τDecay (comp.) [ms]	MEJC Amplitude [nA]	Rs [KΩcm^2]	Cs [μF/cm^2]
CS	48.9 ± 0.9	84.8 ± 3.8	8.9 ± 0.9	9.8 ± 0.6	0.40 ± 0.06 (0.40 ± 0.10)	6.64 ± 1.4	7.6 ± 0.8
dlg^{v59}	103.1 ± 3.6	154.1 ± 5.7	8.1 ± 0.9	11.8 ± 1.1	0.47 ± 0.01 (0.47 ± 0.08)	8.48 ± 2.2	6.6 ± 1.1
dlg^{m52}	96.9 ± 4.4	161.4 ± 4.6	8.2 ± 1.4	10.8 ± 2.3	0.48 ± 0.02 (0.49 ± 0.10)		
dlg^{m52}; post-dlg	93.7 ± 1.4	159.6 ± 5.9	10.0 ± 1.6	8.3 ± 2.1	0.45 ± 0.03 (0.46 ± 0.08)		
dlg^{m52}; pre-dlg	58.6 ± 8.6	104.4 ± 10.4	6.8 ± 2.6	12.3 ± 1.8	0.45 ± 0.03 (0.42 ± 0.07)		

Results are expressed as mean ± SEM. The pooled mean EJC amplitude ± variance is expressed in parenthesis. τ decay corresponds to the EJC decay time constant assuming a single exponential model.